

# Dose-volume consistency and radiobiological characterization between prostate IMRT and VMAT plans

James C. L. Chow<sup>1,2</sup>, Runqing Jiang<sup>3,4</sup>, Alexander Kiciak<sup>4</sup>

<sup>1</sup>Radiation Medicine Program, Princess Margaret Cancer Centre, University Health Network, Toronto, ON, Canada

<sup>2</sup>Department of Radiation Oncology, University of Toronto, Toronto, ON, Canada

<sup>3</sup>Department of Medical Physics, Grand River Regional Cancer Centre, Kitchener, ON, Canada

<sup>4</sup>Department of Physics and Astronomy, University of Waterloo, Waterloo, ON, Canada

Received May 31, 2016; Revised December 04, 2016; Accepted December 05, 2016; Published Online December 26, 2016

## Original Article

### Abstract

**Purpose:** Dose-volume consistency of the planning target volume (PTV) and rectum for the prostate intensity modulated radiotherapy (IMRT) and volumetric modulated arc therapy (VMAT) plans were evaluated and compared. Dependences of radiobiological parameters of the prostate and rectum on the PTV and rectal volume were also investigated. **Methods:** From 40 prostate IMRT and 50 VMAT patients treated with the same prescription (78 Gy per 39 fractions) and dose-volume criteria in the inverse planning, the prostate tumour control probability (TCP), rectal equivalent uniform dose (EUD) and rectal normal tissue complication probability (NTCP) were calculated. The dose-volume consistency of the PTV and rectum, demonstrating the variability of dose-volume histogram (DVH) among patients, was defined and calculated as per the deviation between the corresponding and mean DVH. **Results:** For the IMRT plans, the prostate TCP was found increasing with the PTV with a rate equal to  $1.05 \times 10^{-3} \% \text{ cm}^{-3}$ , which was lower than  $1.11 \times 10^{-3} \% \text{ cm}^{-3}$  for the VMAT plans. Both the rectal EUD and rectal NTCP were found decreasing with the rectal volume. The decrease rates for the IMRT plans (EUD =  $0.47 \times 10^{-3} \text{ Gy cm}^{-3}$  and NTCP =  $3.94 \times 10^{-2} \% \text{ cm}^{-3}$ ) were higher than those for the VMAT (EUD =  $0.28 \times 10^{-3} \text{ Gy cm}^{-3}$  and NTCP =  $2.61 \times 10^{-2} \% \text{ cm}^{-3}$ ). **Conclusion:** For the dose-volume consistency, small prostate TCP variation could be achieved by decreasing the dose-volume variability among the IMRT and VMAT plans. However, dependences of the rectal EUD and rectal NTCP on the dose-volume variability were not significant. It is concluded that maintaining a good dose-volume consistency in prostate plans can decrease the prostate TCP variation among the IMRT and VMAT patients. However, dose-volume variability is not affected by variations of the rectal EUD and rectal NTCP.

**Keywords:** Prostate IMRT, Prostate VMAT, Dose-volume histogram, Prostate TCP, Rectal NTCP, Rectal EUD.

## 1. Introduction

In external beam prostate cancer treatment, intensity modulated radiotherapy (IMRT) has been widely used to replace the 3D-conformal radiotherapy.<sup>1-4</sup> The step-and-shoot IMRT used multiple static photon beams with intensity modulated segmental fields to produce highly conformal dose coverage of the prostate planning target volume (PTV), while sparing the critical organs including the rectum, bladder and femoral head.<sup>5, 6</sup> Recently, volumetric modulated arc therapy (VMAT) becomes popular in prostate radiotherapy.<sup>7, 8</sup> Instead of

sequencing a group of static beam segments produced by the multi-leaf collimator (MLC) in the IMRT, the VMAT technique employs a dynamic MLC approach,<sup>9</sup> in which the MLC aperture, dose rate and gantry angle can simultaneously be changing in a photon arc.<sup>10-12</sup> Since only one to two photon arcs typically are required instead of multiple (5 – 9) photon beams in prostate radiotherapy, one fraction of VMAT can be delivered faster than that of IMRT.<sup>13, 14</sup> However, since VMAT delivery interplays the MLC field, MLC leaf speed, dose

**Corresponding author:** James C. L. Chow; Radiation Medicine Program, Princess Margaret Cancer Centre, University Health Network, M5G 2M9, Ontario, Toronto, Canada.

**Cite this article as:** Chow JC, Jiang R, Kiciak A. Dose-volume consistency and radiobiological characterization between prostate IMRT and VMAT plans. *Int J Cancer Ther Oncol.* 2016; 4(4):447. DOI: 10.14319/ijcto.44.7

rate and gantry speed in the treatment, more complex patient specific quality assurance is needed.<sup>15,16</sup> For the dose distribution in treatment planning, studies showed that prostate VMAT has comparable PTV dose coverage with IMRT.<sup>17-19</sup> Moreover, some studies found that prostate VMAT has improved rectal, bladder and femoral head sparing compared to IMRT.<sup>20-22</sup>

To date, with the rapid development of treatment planning database and toolbox for plan evaluation, studies are conducted to investigate how the treatment planning quality assurance can be benefited by the previously treated plans using similar protocol and delivery technique.<sup>23, 24</sup> There are studies on knowledge-based planning methods that standardizing the automatic radiation treatment plans with a reduction of plan quality variability.<sup>25-27</sup> Results of the above studies lead to a developed model-based treatment planning methods that required inputs from a patient anatomy and prior treatment planning knowledge. In addition, the feasibility of using the knowledge-based planning database to adapt the prostate treatment plan from one institute to a set of cases from an independent clinic was examined.<sup>27,28</sup> The aim of using the knowledge-based planning model is to develop a cross-institutional group that reduces the poor systematic plan quality at institutions with limited prostate IMRT/VMAT experience.

Apart from using results from previously treated plans based on the knowledge-based model, dose-volume results in treatment plans such as dose-volume histograms (DVHs) from previously treated plans are used to compare with a new plan in quality assurance.<sup>24, 29</sup> Dose-volume consistency in a prostate plan can be maintained if the deviation of DVHs between the mean curve of the previously treated plans and the new plan is small, indicating a low planning quality variability. In this case, the planning database is used to maintain a dose-volume consistency in the treatment plan quality assurance. So that every patient is treated with the expected dose-volume characteristics based on the same dose delivery technique in the institution.<sup>28</sup>

In this study, the dose-volume consistency in prostate radiotherapy was evaluated and compared between the IMRT and VMAT plans. Moreover, dependences of the dose-volume consistency on radiobiological parameters such as the prostate tumour control probability (TCP), rectal equivalent uniform dose (EUD) and rectal normal tissue complication probability (NTCP) were determined and investigated. Relationships among the above radiobiological parameters, PTV and rectal volume were compared between the IMRT and VMAT plans.

## 2. Methods and Materials

### 2.1. Patient data

Forty and fifty prostate patients treated with IMRT and VMAT at the Grand River Regional Cancer Centre in Grand River Hospital were used in this study. All patients were treated with the same prescription dose (78 Gy in 39 fractions, 2 Gy per fraction) with no lymph nodes and semi-vesicle targeted.

### 2.2. Treatment planning and dose delivery

All IMRT and VMAT treatment plans were created using the Pinnacle<sup>3</sup> (Philips Medical Systems, Andover, MA) and Eclipse treatment planning system (Varian Medical System, Palo Alto, CA). Dose delivery was carried out by a Varian 21 EX linear accelerator (Varian Medical System, Palo Alto, CA) equipped with a 120-leaf Millennium MLC system to generate beam segments for beam intensity modulation. Patient specific dosimetry quality assurance measurements for the IMRT were performed by the MapCHECK<sup>®</sup> system (Sun Nuclear Corp., Melbourne, FL), while for the VMAT were performed by the ArcCHECK<sup>®</sup> (Sun Nuclear Corp., Melbourne, FL) and Delta4 system (ScandiDos Inc., Madison, WI).

For each patient in the IMRT or VMAT plan, the prostate, rectum, bladder, left and right femoral head were contoured in his computed tomography (CT)-simulation image set. The gross and clinical target volume (GTV and CTV) were equal to the prostate volume, while the PTV was created by expansion of the CTV with 1 cm except 0.7 cm posteriorly. Both IMRT and VMAT plans used the same dose-volume criteria as shown in Table 1 in the inverse planning optimization. For the prostate IMRT plan, the seven-beam technique was used with beam energy equal to 6 MV, and beam angles equal to 40°, 80°, 110°, 250°, 280°, 310° and 355°. For the prostate VMAT plan, a single 360° photon arc was used. The VMAT plan was inversely optimized by the Eclipse RapidArc algorithm (Varian Medical System, Palo Alto, CA).

**Table 1:** Dose-volume criteria used in the IMRT and VMAT prostate plans.

Volume of interest	Dose-volume criteria (Gy)
CTV	$D_{99\%} \geq 78$
PTV	$D_{99\%} \geq 74.1$
PTV	Maximum dose to 1 cm <sup>3</sup> ≤ 81.9
Rectum	$D_{30\%} \leq 70$
Rectum	$D_{50\%} \leq 54.3$
Bladder	$D_{30\%} \leq 70$
Bladder	$D_{50\%} \leq 54.3$
Left and Right Femoral Head	$D_{5\%} \leq 54.3$

### 2.3. Calculations of the prostate TCP, rectal EUD and rectal NTCP

The prostate TCP was calculated by the following equation:

$$TCP = \frac{\exp(p + qD)}{1 + \exp(p + qD)} \quad (1)$$

In this logistic regression equation,  $D$  is the dose. Parameters  $p$  and  $q$  are related to the  $D_{50}$  and the normalized slope at the point of 50% control probability,  $\gamma_{50}$ . Information of  $D_{50}$  and  $\gamma_{50}$  can be found from Okunieff *et al* summarized related clinical data for a variety of tumours and reported parameters.<sup>30</sup> From Eq. (1), control probability for the tumourlet,  $TCP(v_i, D_i)$ , with volume  $v$  and dose  $D$  can be inferred from the TCP for the whole volume using the following equation:

$$TCP(v_i, D_i) = TCP(D_i)^{v_i} \quad (2)$$

In Eq. (2),  $(v_i, D_i)$  represents the differential DVH.

The phenomenological model suggested by Niemierko was used to calculate the generalized EUD of the rectum.<sup>31</sup> The equation based on the power law behavior of tissue response is as follows:

$$EUD = \left( \sum_{i=1}^n (v_i D_i^a) \right)^{\frac{1}{a}} \quad (3)$$

In Eq. (3),  $a$  is a biological parameter specified to a normal tissue. Parameter  $v_i$  is the  $i^{th}$  partial volume receiving dose  $D_i$  (Gy). Parameters  $a$  and  $v_i$  have no unit. The  $D_i$  and  $v_i$  data pairs were determined from the differential DVH of the rectum. It should be noted that the sum of all partial volumes  $v_i$  is equal to one because the relative volume of the whole volume of interest is equal to one. The value of  $a$  for rectum is set to 24 in this study.<sup>32</sup>

The rectal NTCP was calculated based on the Lyman-Burman-Kutcher algorithm:<sup>33-35</sup>

$$NTCP = \frac{1}{2\pi} \int_{-\infty}^t e^{\frac{-x^2}{2}} dx \quad (4)$$

, and

$$t = \frac{D - TD_{50}(v)}{mTD_{50}(v)} \quad (5)$$

In Eq. (5),  $v = V/V_{ref}$  and  $TD_{50}(v) = TD_{50}(1) v^n$ , as suggested by Burman *et al*,<sup>34</sup> a  $TD_{50}$  of 80 Gy, an  $n$  of 0.12, and  $m$  of 0.15 were used for rectum here. The prostate TCP, rectal EUD and rectal NTCP were determined using an in-house program developed on the MATLAB platform by converting the cumulative DVH to differential DVH.<sup>36</sup>

### 2.4. Estimation of the dose-volume consistency

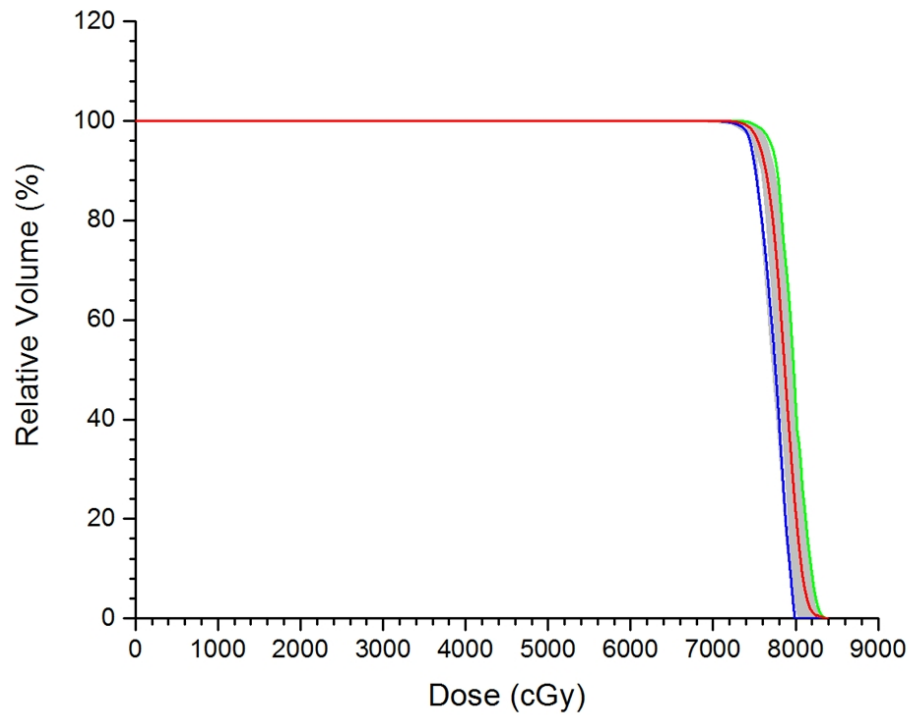
The consistency of the DVH is estimated by the following equation:

$$\sigma = \frac{1}{n} \sum_{i=1}^n |v_{mean_i}(D_{mean_i}) - v_i(D_i)| \quad (6)$$

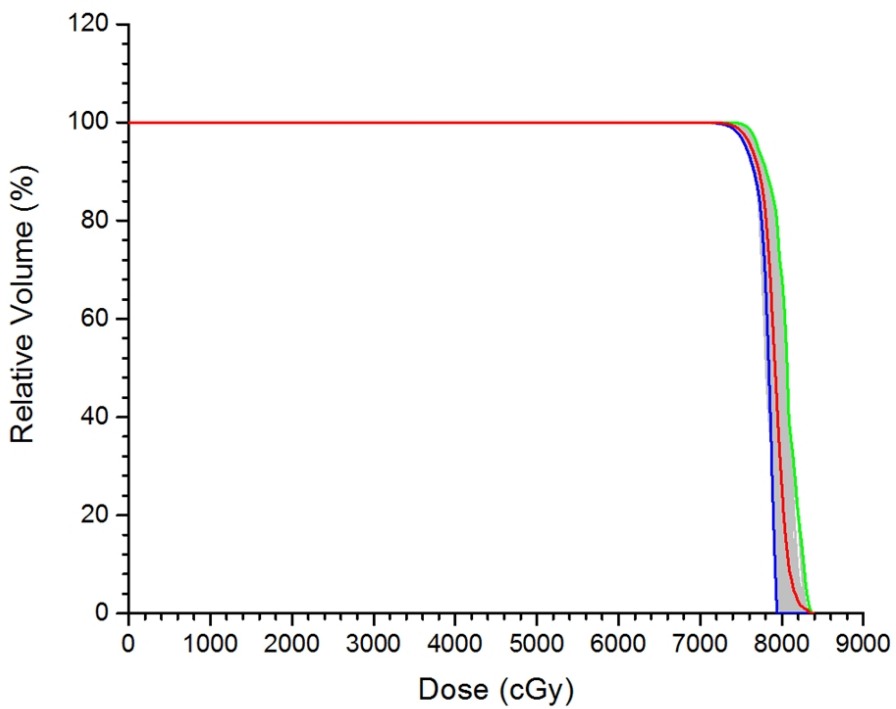
where  $\sigma$  is the dose-volume variability based on the DVH relative to its mean.  $v_{mean_i}$  and  $D_{mean_i}$  are the relative volume and dose data pairs of the mean DVH curve in the database, while  $v_i$  and  $D_i$  are the corresponding data pairs of the DVH curve being estimated.  $n$  is the number of dose bin in the DVH. It can be seen that when the estimated DVH curve is the same as the mean curve,  $\sigma$  becomes zero according to the Eq. (6), and there is no dose-volume variability in the target or normal tissue of interest.

## 3. Results

Figures 1(a) and 1(b) show DVHs of the PTV and rectum for all prostate IMRT patients, while Figures 2(a) and 2(b) show DVHs of the PTV and rectum for all VMAT patients. In Figures 1 and 2, the corresponding mean DVH curves were calculated and are shown in red color in the figures. The curves for the mean  $\pm 2 \times$  standard deviation were also plotted and are shown in green and blue color in Figures 1 and 2. Dependence of the prostate TCP on the PTV is shown in Figure 3, while dependences of the rectal EUD and rectal NTCP on the rectal volume are shown in Figures 4(a) and 4(b). For the dose-volume consistency, dependence of the prostate TCP on the dose-volume variability is shown in Figure 5. Figures 6(a) and 6(b) show dependences of the rectal EUD and rectal NTCP on the dose-volume variability. All calculations in Figures 3 – 6 are based on one fraction of treatment dose equal to 2 Gy. The straight lines in Figures 3 and 4 are results of linear fitting according to the corresponding data points.

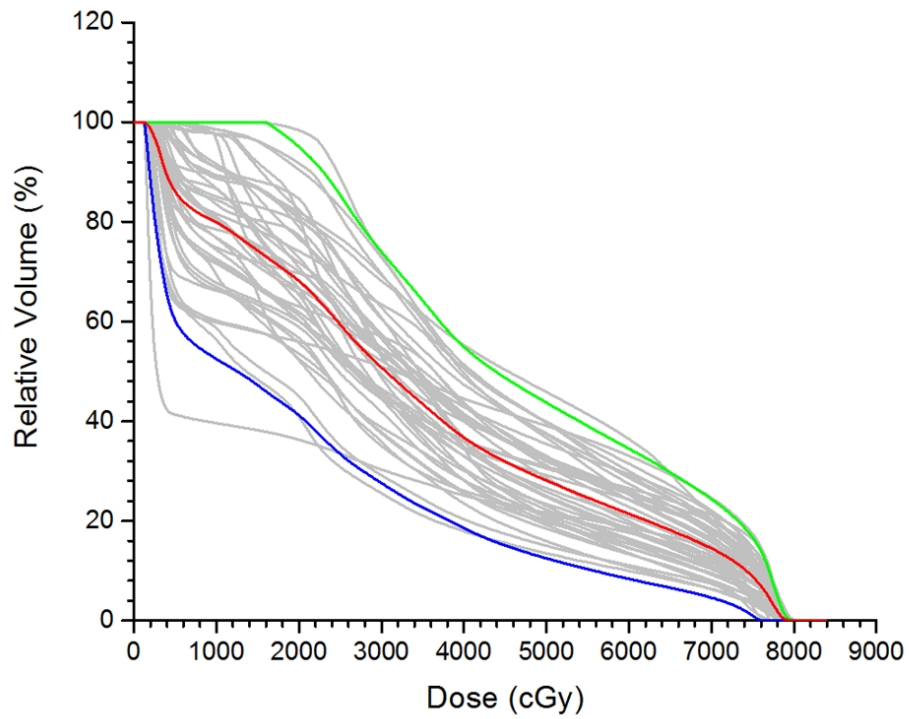


a)

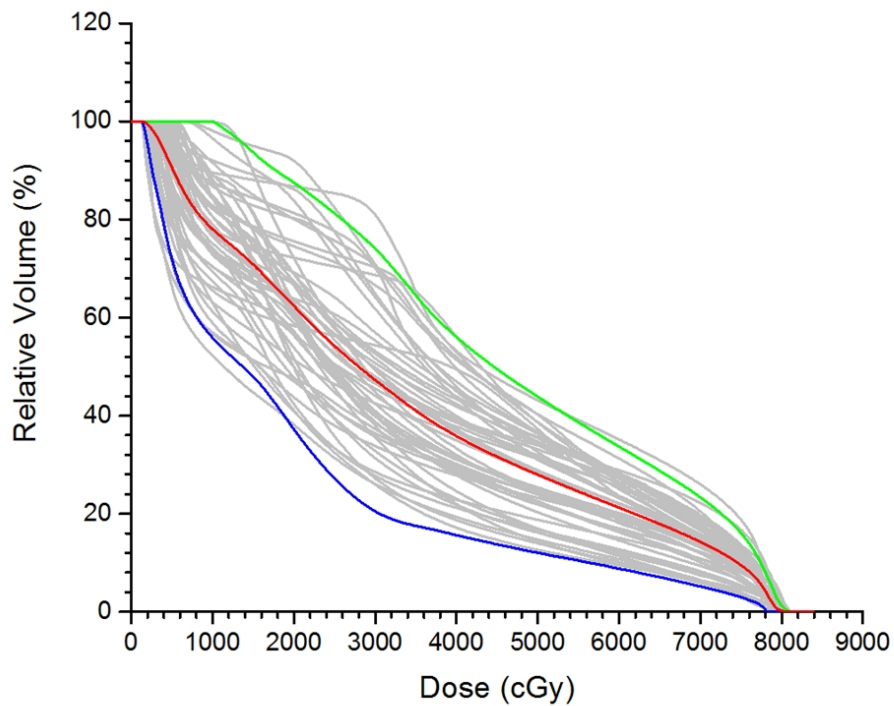


b)

**Figure 1:** DVHs of the PTV for all (a) IMRT and (b) VMAT prostate plans with the mean, mean + 2 × standard deviation, and mean - 2 × standard deviation curves in red, green and blue color, respectively.

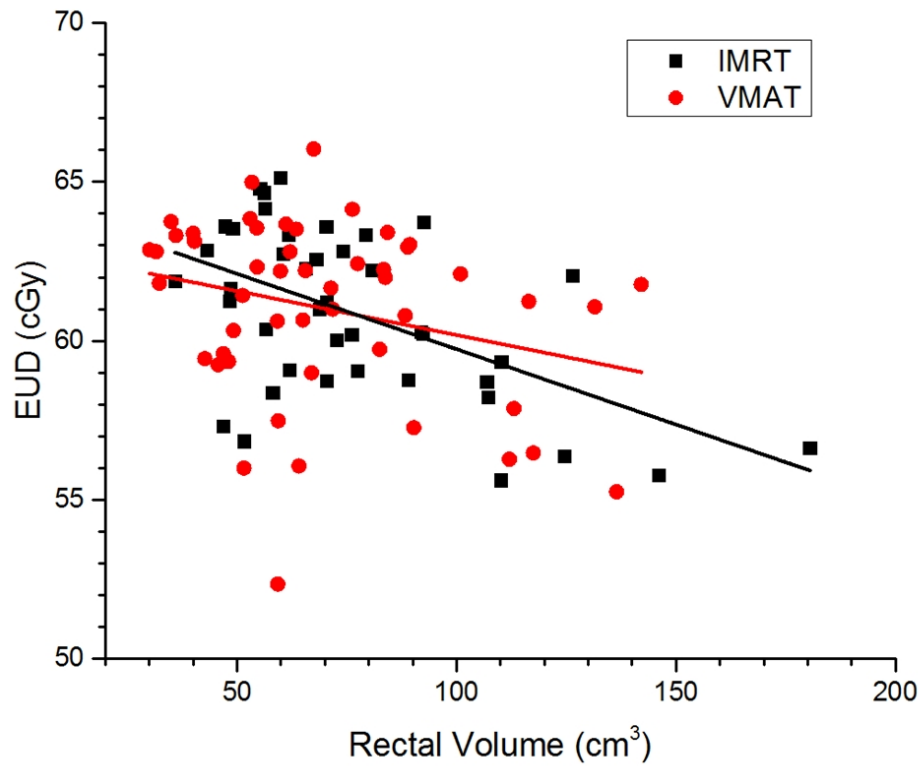


a)

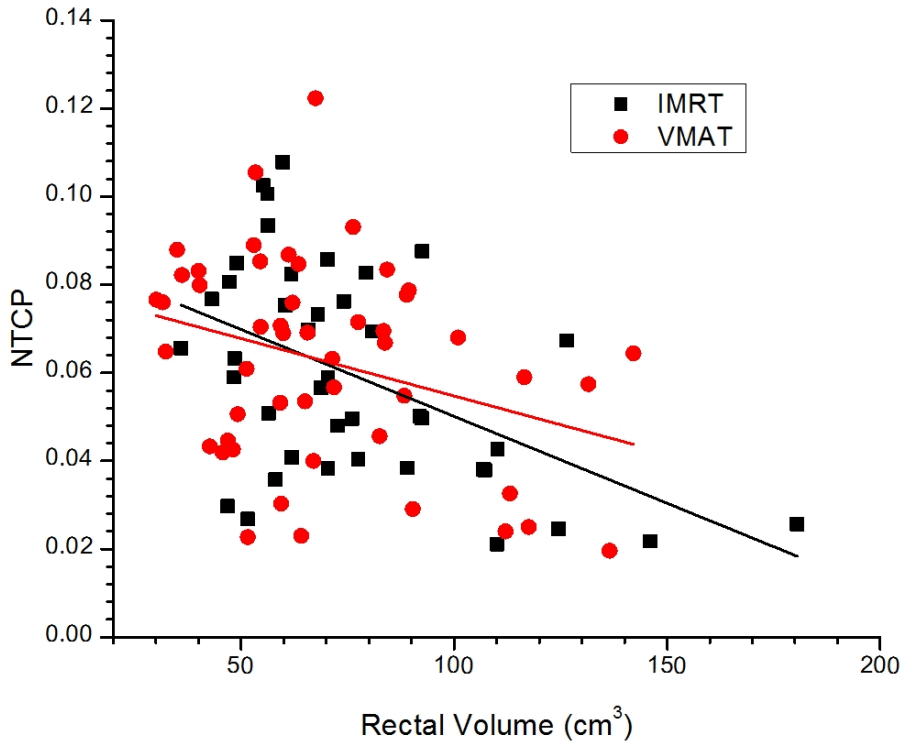


b)

**Figure 2:** DVHs of the rectum for all (a) IMRT and (b) VMAT prostate plans with the mean, mean + 2 × standard deviation, and mean - 2 × standard deviation curves in red, green and blue color, respectively.



(a)



b)

**Figure 4:** Rectal (a) EUD and (b) NTCP vs. rectal volume for all IMRT and VMAT plans.

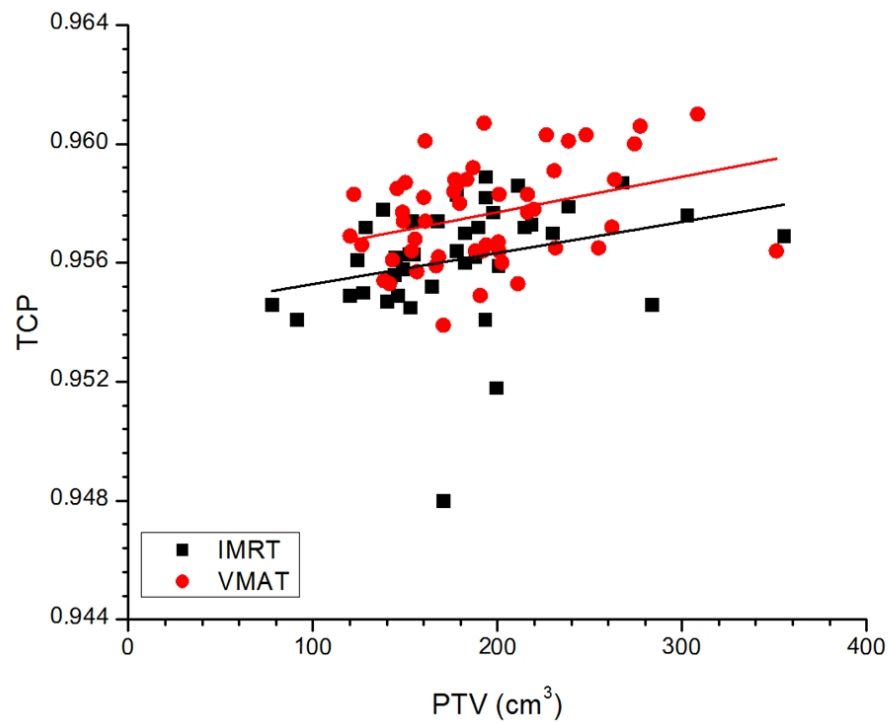


**Figure 3:** Relationship between the prostate TCP and PTV for all IMRT and VMAT plans.

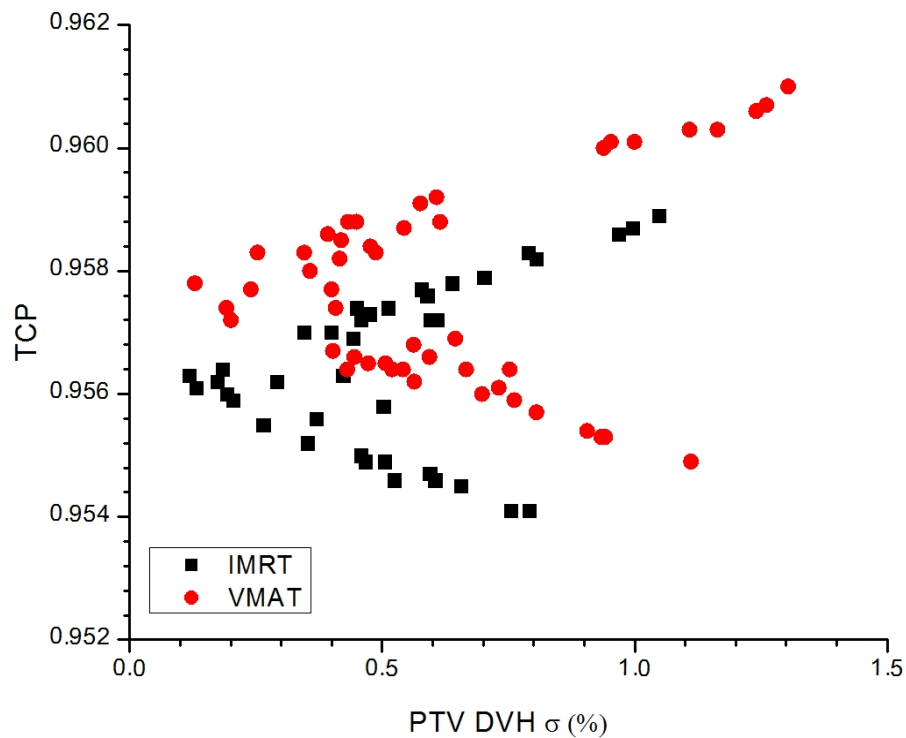
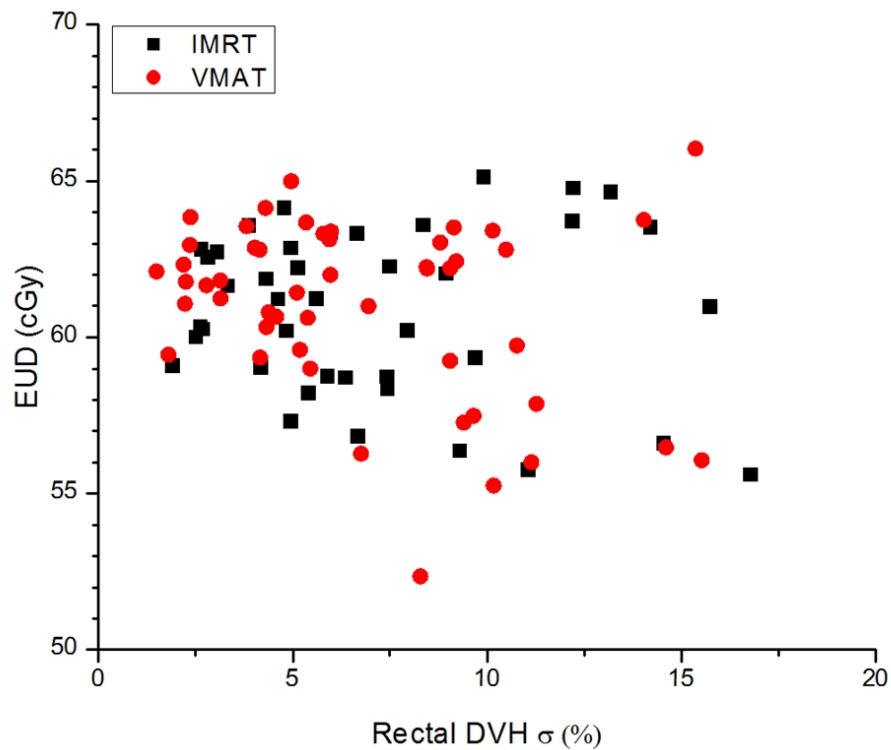
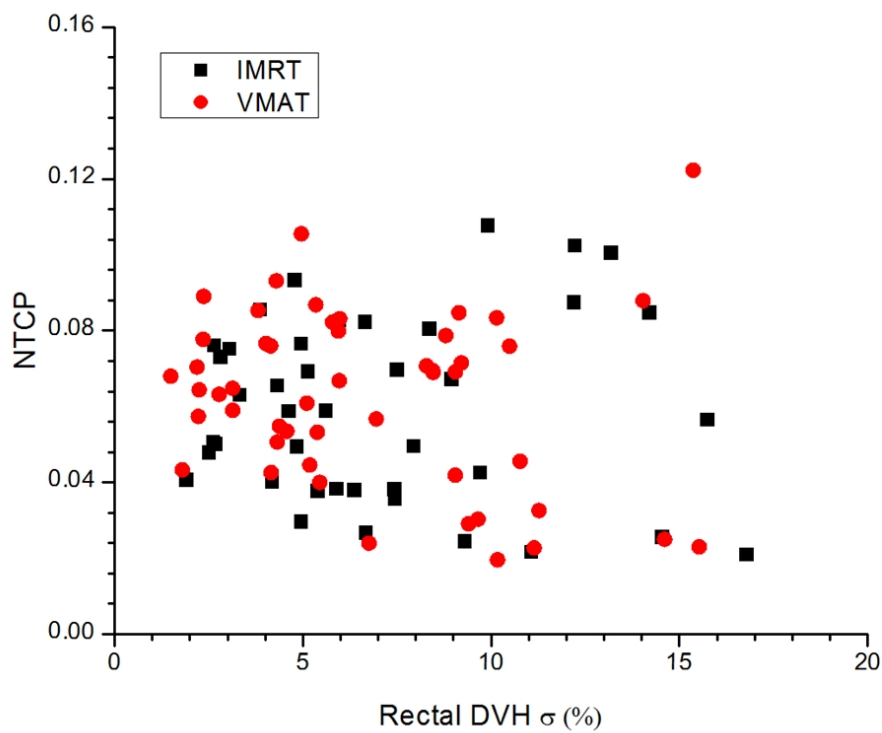


**Figure 5:** Relationship between the prostate TCP and dose-volume variability for all IMRT and VMAT plans.





a)



b)

**Figure 6:** Relationship between the rectal (a) EUD and (b) NTCP and the dose-volume variability for all IMRT and VMAT plans.



## 4. Discussion

### 4.1. DVHs of the PTV and rectum

In Figures 1(a) and 1(b), it is seen that most DVH curves of the prostate PTV are within the mean DVH curve  $\pm 2 \times$  standard deviation. For the mean DVH curves of the PTV, the  $D_{99\%}$ ,  $D_{95\%}$  and  $D_{5\%}$  for the IMRT plans are 74.12 Gy, 75.61 Gy and 81.25 Gy, which have no significant deviation compared to those for the VMAT plans ( $D_{99\%}$ ,  $D_{95\%}$  and  $D_{5\%}$  = 74.45 Gy, 76.25 Gy, and 81.45 Gy). Moreover, the mean dose of the PTV for the VMAT plans is 79.05 Gy which is slightly higher than that for the IMRT plans (78.63 Gy). In this study, all plans were approved based on the specific dose-volume criteria (Table 1) with patient specific dosimetry quality assurance passed.

For the DVH curves of the rectums in Figures 2(a) and 2(b), the mean DVH curves for the IMRT and VMAT plans are shown together with the curves  $\pm 2 \times$  standard deviation. It can be seen that most DVH curves of the rectums are enveloped between the mean curves  $\pm 2 \times$  standard deviation. For the mean DVH curves of the rectums, the  $D_{30\%}$  and  $D_{50\%}$  for the IMRT plans are 47.4 Gy and 30.5 Gy, which are slightly higher than those for the VMAT ( $D_{30\%}$  and  $D_{50\%}$  = 47.1 Gy and 27.9 Gy). The  $V_{30Gy}$  and  $V_{38Gy}$  for the IMRT plans are also higher (62.44% and 51.4%) than those for the VMAT (56.7% and 47.8%), and the mean dose of the rectum is 35.27 Gy for the IMRT plans compared to 33.91 Gy for the VMAT.

### 4.2. Dependences of the prostate TCP on the PTV, and rectal EUD and rectal NTCP on the rectal volume

Figure 3 shows the relationship between the prostate TCP and PTV for the IMRT and VMAT plans. In Figure 3, it can be seen that the prostate TCP slightly increases with the PTV for both the IMRT and VMAT plans. According to the slopes of lines in data fitting, the rate of prostate TCP increased with PTV for the IMRT plans is  $1.05 \times 10^{-3} \% \text{ cm}^{-3}$ , compared to  $1.11 \times 10^{-3} \% \text{ cm}^{-3}$  for the VMAT. Moreover, the mean prostate TCP for the VMAT plans is about 0.16 % higher than the IMRT. This indicates that slightly higher prostate TCP can be achieved by using the VMAT technique compared to the IMRT.

Dependences of the rectal EUD on the rectal volume are shown in Figure 4(a) for the IMRT and VMAT plans. It is seen in Figure 4(a) that the rectal EUD of both the IMRT and VMAT plans decrease with an increase of the rectal volume. From the straight lines plotted based on data fitting, slopes of lines for the IMRT and VMAT plans are  $0.47 \times 10^{-3} \text{ Gy cm}^{-3}$  and  $0.28 \times 10^{-3} \text{ Gy cm}^{-3}$ , respectively. That is, the variation of rectal EUD on the rectal volume is more sensitive to the IMRT plans than the VMAT. Similar relationship can be found in Figure 4(b) showing the dependences of the rectal NTCP on the rectal volume. The rectal NTCP decreases with an increase of

rectal volume in a rate equal to  $3.94 \times 10^{-2} \% \text{ cm}^{-3}$  and  $2.61 \times 10^{-2} \% \text{ cm}^{-3}$ , for the IMRT and VMAT plans, respectively. Again, variation of the rectal NTCP on the rectal volume is more sensitive to the IMRT plans than the VMAT.

### 4.3. Dependences of the prostate TCP, rectal EUD, rectal NTCP on the dose-volume variability

The prostate TCP is plotted against the dose-volume variability,  $\sigma$  calculated from the Eq. (6) based on DVHs of the PTV from the IMRT and VMAT plans, as shown in Figure 5. It is seen in Figure 5 that the prostate TCP for the VMAT plans is higher than that of the IMRT, which agrees with Figure 3. The mean prostate TCP for the IMRT plans is 95.61% which is lower than 95.76% for the VMAT. When the value of  $\sigma$  is close to zero, which means the dose-volume consistency is high, the variation range of the prostate TCP is small. This reveals that a high dose-volume consistency can ensure a small prostate TCP variation in both the IMRT and VMAT plans.

Figures 6(a) and 6(b) show the dependences of the rectal EUD and rectal NTCP on the dose-volume variability for the IMRT and VMAT plans. In Figure 6, it is seen that though there is a slight increase of rectal EUD and rectal NTCP range with a decrease of dose-volume consistency, the deviation of data between the IMRT and VMAT plans is not significant. It is found from the figure that the dependences of the rectal EUD and rectal NTCP on the dose-volume consistency are very similar for the IMRT and VMAT plans. This shows that both the IMRT and VMAT plans have similar variations of the rectal EUD and rectal NTCP on the dose-volume consistency.

## 5. Conclusion

Dependences of dose-volume consistency on the prostate TCP, rectal EUD and rectal NTCP were evaluated and compared between the IMRT and VMAT plans. In addition, variations of the above radiobiological parameters on the PTV and rectal volume were studied. It is found that while the prostate TCP increased with the PTV, the rectal EUD and rectal NTCP decreased with an increase of the rectal volume. The variation rates of the rectal EUD and rectal NTCP were higher for the IMRT plans than VMAT. For dependences of the prostate dose-volume consistency, it is concluded that a small prostate TCP variation can be maintained by decreasing the dose-volume variability. However, variations of the rectal dose-volume consistency on the rectal EUD and rectal NTCP were found not significant for both the IMRT and VMAT plans.

## Conflict of interest

The authors declare that they have no conflicts of interest. The authors alone are responsible for the content and writing of the paper.

## Funding

Nil.

## Acknowledgement

The authors would like to thank Dr Muhammad Isa Khan in the University of Gujrat, Pakistan for some of the dose-volume calculations. All treatment plans were created with patients in the Grand River Regional Cancer Centre, Grand River Hospital, Kitchener, Ontario, Canada.

## References

1. Hummel S, Simpson EL, Hemingway P, *et al.* Intensity-modulated radiotherapy for the treatment of prostate cancer: a systematic review and economic evaluation. *Health Technol Assess.* 2010;14:1-108.
2. Hall EJ, Wu C. Radiation-induced second cancers: the impact of 3D-CRT and IMRT. *Int. J. Radiation Oncology Biol. Phys.* 2003;56:83-8.
3. Zelefsky MJ, Chan H, Hunt M, *et al.* Long-term outcome of high dose intensity modulated radiation therapy of patients with clinically localized prostate cancer. *J Urology.* 2006;176:1415-9.
4. Veldeman L, Madani I, Hulstaert F, *et al.* Evidence behind use of intensity-modulated radiotherapy: a systematic review of comparative clinical studies. *Lancet Oncol.* 2008;9:367-5.
5. Adams EJ, Convery DJ, Cosgrove VP *et al.* Clinical implementation of dynamic and step-and-shoot IMRT to treat prostate cancer with high risk of pelvic lymph node involvement. *Radiother Oncol.* 2004;70:1-10.
6. Grigorov GN, Chow JCL, Barnett RB. Dosimetry limitations and a dose correction methodology for step-and-shoot IMRT. *Phys Med Biol.* 2006;51:637-52.
7. Otto K. Volumetric modulated arc therapy: IMRT in a single gantry arc. *Med. Phys.* 2008;35:310-7.
8. Yu CX. Intensity-modulated arc therapy with dynamic multileaf collimation: an alternative to tomotherapy. *Phys. Med. Biol.* 1995;40:1435-9.
9. Chow JCL, Grigorov GN, Yazdani N. SWIMRT: a graphical user interface using sliding window algorithm to construct a fluence map machine file. *J Appl Clin Med Phys.* 2006;7:69-85.
10. Rao M, Yang W, Chen F, *et al.* Comparison of Elektra VMAT with helical tomotherapy and fixed field IMRT: Plan quality, delivery efficiency and accuracy. *Med. Phys.* 2010;37:1350-59.
11. Cao D, Afghan MKN, Ye J, *et al.* A generalized inverse planning tool for volumetric modulated arc therapy. *Phys. Med. Biol.* 2009;54:6725-38.
12. Shepard DM, Cao D, Afghan MKN, *et al.* An arc-sequencing algorithm for intensity modulated arc therapy. *Med. Phys.* 2007;34:464-70.
13. Chow JCL, Jiang R. Dosimetry estimation on variations of patient size in prostate volumetric-modulated arc therapy. *Med. Dosim.* 2013;38:42-7.
14. Chow JCL, Jiang R. Prostate volumetric-modulated arc therapy: dosimetry and radiobiological model variation between the single-arc and double-arc technique. *J Appl Clin Med Phys.* 2013;14:3-12.
15. Letourneau D, Publicover J, Kozelka J, *et al.* Novel dosimetric phantom for quality assurance of volumetric modulated arc therapy. *Med. Phys.* 2009;36:1813-21.
16. Haga A, Nakagawa K, Shiraishi K, *et al.* Quality assurance of volumetric modulated arc therapy using Elekta Synergy. *Acta Oncol.* 2009;48:1193-7.
17. Chow JCL, Jiang R. Comparison of dosimetric variation between prostate IMRT and VMAT due to patient's weight loss: Patient and phantom study. *Rep Pract Oncol Radiother.* 2013;18:272-8.
18. Davidson MTM, Blake SJ, Batchelar DL, *et al.* Assessing the role of volumetric modulated arc therapy (VMAT) relative to IMRT and helical tomotherapy in the management of localized, locally advanced, and post-operative prostate cancer. *Int. J. Radiation Oncology Biol. Phys.* 2011;80:1550-8.
19. Hardcastle N, Tome WA, Foo K, *et al.* Comparison of prostate IMRT and VMAT biologically optimized treatment plans. *Med. Dosim.* 2011;36:292-8.
20. Iori M, Cattaneo G, Cagni E, *et al.* Dose-volume and biological-model based comparison between helical tomotherapy and (inverse-planned) IMAT for prostate tumours. *Radiother Oncol.* 2008;88:34-45.
21. Zhang P, Happersett L, Hunt M, *et al.* Volumetric modulated arc therapy: planning and evaluation for prostate cancer cases. *Int. J. Radiation Oncology Biol. Phys.* 2010;76:1456-2.
22. Wolff D, Stieler F, Welzel G, *et al.* Volumetric modulated arc therapy (VMAT) vs. serial tomotherapy, step-and-shoot IMRT and

- 3D-conformal RT for treatment of prostate cancer. *Radiother Oncol.* 2009;93:226–33.
23. Wu B, Ricchetti F, Sanguineti G *et al.* Patient geometry-driven information retrieval for IMRT treatment plan quality control. *Med Phys.* 2009;36:5497-505.
  24. Chow JCL. Radiation treatment planning based on big data of previously treated plans using the Gaussian error function model. Proceedings, HPCS 2015, Advanced Computing and Big Data: Driving Competitiveness and Discovery. 2015:12.
  25. Chanyavanich V, Das SK, Lee WR, *et al.* Knowledge-based IMRT treatment planning for prostate cancer. *Med Phys.* 2011;38:2512-22.
  26. Good D, Lo J, Lee WR, *et al.* A knowledge-based approach to improving and homogenizing intensity modulated radiation therapy planning quality among treatment centers: an example application to prostate cancer planning. *Int J Radiat Oncol Biol Phys.* 2013;87:176-81.
  27. Nwankwo O, Mekdash H, Shihono DSK, *et al.* Knowledge-based radiation therapy (KBRT) treatment planning versus planning by experts: validation of a KBRT algorithm for prostate cancer treatment planning. *Radiat Oncol.* 2015;10:111.
  28. Nelms BE, Robinson G, Markham J, *et al.* Variation in external beam treatment plan quality: An inter-institutional study of planners and planning systems. *Pract Radiat Oncol.* 2012;2:296-305.
  29. Zhu X, Ge Y, Li T, *et al.* A planning quality evaluation tool for prostate adaptive IMRT based on machine learning. *Med Phys.* 2011;38:719-26.
  30. Okunieff P, Morgan D, Niemierko A, *et al.* Radiation dose response of human tumours. *Int J Radiat Oncol Biol Phys.* 1995;32:1227-37.
  31. Niemierko A. A generalized concept of equivalent uniform dose (EUD). *Med Phys.* 1999;26:1100.
  32. Shan W, Chow JCL, Markel D, *et al.* Rectal equivalent uniform dose analysis on the prostate IMRT for interfraction organ motion using the Gaussian error function. *Med Phys.* 2011;38:3640.
  33. Lyman JT. Complication probability as assessed from dose-volume histogram. *Radiat Res.* 1985;104:S13-19.
  34. Burman C, Kutcher GJ, Emami B, *et al.* Fitting of normal tissue tolerance data to an analytic function. *Int J Radiat Oncol Biol Phys.* 1991;21:123-35.
  35. Kutcher GJ, Burman C, Brewster L, *et al.* Histogram reduction method for calculating complication probability for three-dimensional treatment planning evaluation. *Int J Radiat Oncol Biol Phys.* 1991;21:137-46.
  36. Jiang R, Barnett RB, Chow JCL, *et al.* The use of spatial dose gradients and probability density function to evaluate the effect of internal organ motion for prostate IMRT treatment planning. *Phys Med Biol.* 2007;52:1469-84.